Conformational studies of two new brassinosteroid analogues with a 22,23-*trans* diol function

Susanne Drosihn,[a] Andrea Porzel,[a] Brunhilde Voigt,[a] Wolfgang Brandt,[b] Christoph Wagner,[c] Kurt Merzweiler[c] and Günter Adam*[a]

[a] *Institut für Pflanzenbiochemie Halle, Weinberg 3, D-06120 Halle/Saale, Germany*
[b] *Fachbereich für Biochemie/Biotechnologie, Martin-Luther-Universität Halle-Wittenberg, Kurt-Mothes-Str. 3, 06120 Halle/Saale, Germany*
[c] *Fachbereich für Chemie, Martin-Luther-Universität Halle-Wittenberg, Kurt-Mothes-Str. 2, 06120 Halle/Saale, Germany*

Received (in Cambridge) 23rd September 1998, Accepted 27th November 1998

22,24-Diepiteasterone (**3**) and 23,24-diepiteasterone (**4**) were synthesized starting from a mixture of the corresponding (22*S*,23*S*)- and (22*R*,23*R*)-epoxides. Using detailed NOE investigations and molecular dynamic simulations with explicit solvent, the preferred conformations of both compounds were determined in solution. For both compounds **3** and **4** a preferred conformation of the side chain was found. For **4**, by X-ray analysis the conformation in crystalline state was determined which differs distinctly from that in solution.

Introduction

Brassinosteroids represent a new class of steroidal phytohormones with high growth-promoting and anti-stress activity as well as other multiple effects on the growth and development of plants.[1] At present, more than 40 native brassinosteroids are known and a lot of synthetic analogues have been synthesized in recent years.[2] Structural variations lie in the substitution pattern of rings A/B and different alkylation at C-24. All hitherto known native brassinosteroids possess a 22*R*,23*R* diol structural feature in the side chain moiety which is essential for high biological activity. Thus, compounds with a 22*R*,23*R*-hydroxy function are much more active than synthetic analogues with 22*S*,23*S* configuration. The fact that brassinosteroids with the 24*S* alkyl group show a tenfold higher bioactivity than corresponding ones with a 24*R* alkyl substitution is a further example of the significance of the stereochemistry at the asymmetric centres in the side chain for bioactivities of these plant hormones.[3] Recently, for the two most important native members brassinolide (**1**) and 24-epibrassinolide (**2**) we

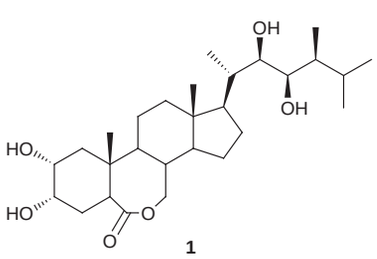

1

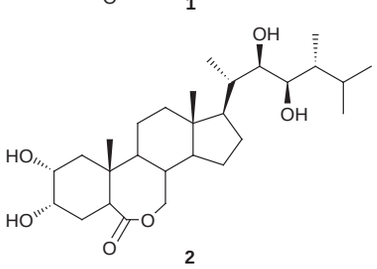

2

have shown distinct differences in the solution side chain conformation, suggesting their relevance for putative hormone–receptor interactions.[4]

In continuation of these studies we report here our investigations on preferential side chain conformations of the two new bisepimeric brassinosteroid analogues (22*S*,24*R*)-teasterone (**3**) and (23*S*,24*R*)-teasterone (**4**) by means of NOE experiments

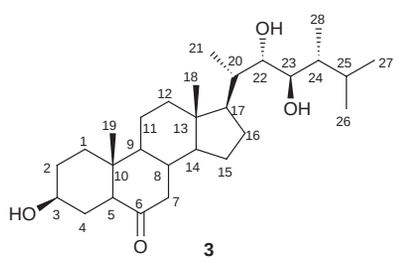

3

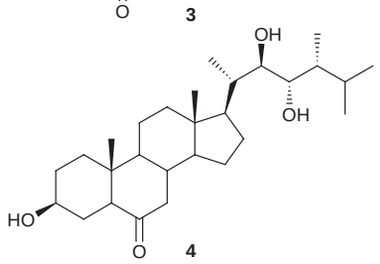

4

and molecular modelling. We were interested in the conformational differences between **3** and **4** and in a comparison of the conformation of these two almost bioinactive compounds[5] with the native brassinosteroids **1** and **2**. In order to determine the side chain conformations we used quantitative NOE measurements followed by force field calculations for structure determination and refinement.

Experimental

General

Melting points are uncorrected. $[\alpha]_D$ values are given in 10^{-1} deg cm^2 g^{-1}, circular dichroic absorptions $\Delta\varepsilon$ are given in cm^2 mmol^{-1}. Preparative and analytical HPLC was carried out on a KNAUER instrument with a YMC column, on ODS, 5 μm, 20 × 150 mm (preparative), 4.6 × 250 mm (analytical), CH_3CN–H_2O as eluent, 5 ml min^{-1} (preparative), 1 ml min^{-1} (analytical) and UV detection at 210 nm. CD spectra were

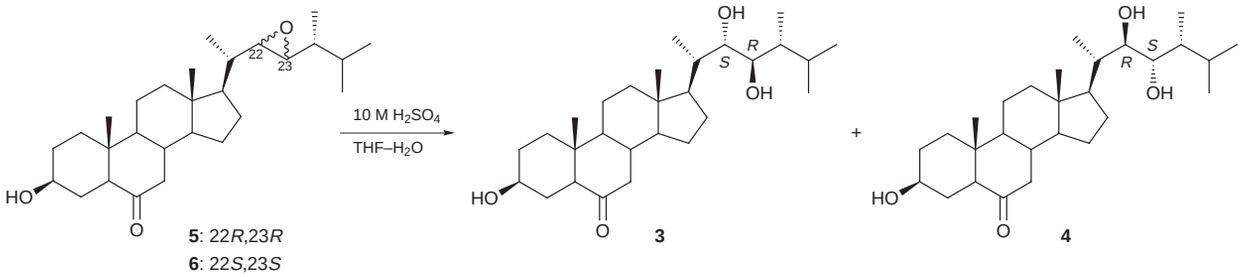

Scheme 1

Table 1 ^{1}H and ^{13}C chemical shifts of compounds **3** and **4** in ($CDCl_3$ unless otherwise noted; *J* values in parentheses are given in Hz)

	3		**4**	
Position	δ_H [a,b]	δ_C	δ_H [a,b]	δ_C [c]
1	*1.23*/*1.77*	36.6	*1.25*/*1.77*	36.6
2	*1.84*/*1.39*	30.7	*1.84*/*1.38*	30.4
3	3.576 tt (11.2/4.7)	70.7	3.580 tt (11.2/4.6)	70.2
4	*1.89*/*1.48*	29.9	*1.90*/*1.46*	29.6
5	2.204 dd (12.5/2.8)	56.7	2.215 dd (12.5/2.8)	56.7
6	—	210.8	—	211.6
7	*1.94*/*2.31*	46.6	*1.96*/*2.32*	46.6
8	*1.78*	37.8	*1.82*	38.0
9	*1.23*	53.9	*1.24*	53.8
10	—	40.5	—	41.0
11	*1.62*/*1.34*	21.4	*1.63*/*1.36*	21.5
12	*1.24*/*2.04*	39.4	*1.26*/*2.03*	39.5
13	—	43.3	—	42.0
14	*1.25*	56.3	*1.29*	56.6
15	*1.55*/*1.10*	24.2	*1.56*/*1.10*	23.8
16	*1.94*/*1.44*	28.1	*1.92*/*1.32*	27.5
17	*1.70*	52.7	*1.51*	52.4
18	0.687 s	11.7	0.710 s	11.9
19	0.756 s	13.0	0.760 s	13.0
20	*1.75*	42.3	*1.87*	36.1
21	1.079 d (6.7)	14.3	0.961 d (6.8)	11.8
22	3.751 dd (8.4/2.6)	74.2	3.546 br d (8.5)	72.7
23	3.622 dd (8.4/4.2)	76.3	3.677 br d (8.5)	72.2
24	*1.67*	40.9	*1.60*	39.6
25	*2.03*	26.9	*1.62*	30.5
26^{proR}	0.887 d (6.8)	18.1	0.966 d (6.4)	21.0
27^{proS}	0.942 d (7.0)	22.5	0.943 d (6.4)	20.0
28	0.926 d (7.3)	10.9	0.871 d (6.7)	9.4

[a] Geminal protons: α/β. [b] Values in *italics* are chemical shifts of HSQC cross-peaks. [c] In $CDCl_3$ + a little CD_3OD.

recorded on a JASCO J-710. EI mass spectra were recorded on an AMD 402 using 70 eV.

Synthesis

A solution of a 1:1 mixture of epoxides **5** and **6**[6] (0.22 g, 0.5 mmol) in THF–H_2O (9:1 v/v, 0.07 l) and H_2SO_4 (10 M, 0.035 l) was stirred for 20 h at room temperature. Removal of the solvent and extraction with ethyl acetate gave a mixture of diastereomeric 22,23-diols **3** and **4**, which were separated by preparative HPLC (CH_3CN–H_2O 7:3, v/v) (see Scheme 1).

(22*S*,23*R*,24*R*)-3β,22,23-Trihydroxy-24-methyl-5α-cholestan-6-one (22,24-diepiteasterone, 3). (0.06 g, 27%), mp 195–197 °C (from acetone–n-hexane) (Found: C, 74.7; H, 10.7. Calc. for $C_{28}H_{48}O_4$: C, 75.0; H, 10.8%); HPLC (CH_3CN–H_2O 9:1, v/v) R_t/min 4.3; $[\alpha]_D^{28}$ −26.0 (*c* 1.0 in CH_3OH); λ_{max}(CH_3OH)/nm 280 (ε/dm^3 mol^{-1} cm^{-1} 180); $\Delta\varepsilon_{294}$ −1.41; ν_{max}(nujol)/cm^{-1} 1700 (C=O), 3276, 3462 and 3625 (OH); *m*/*z* 430 (M^+ − 18, 1%), 377 (M^+ − 71, 2), 359 (M^+ − 89, 3), 348 (M^+ − 100, 100); δ_H and δ_C see Table 1.

(22*R*,23*S*,24*R*)-3β,22,23-Trihydroxy-24-methyl-5α-cholestan-6-one (23,24-diepiteasterone, 4). (0.12 g, 54%), mp 226–227 °C (from acetone–n-hexane) (Found: C, 74.7; H, 10.6. Calc. for $C_{28}H_{48}O_4$: C, 75.0; H, 10.8%); HPLC (CH_3CN–H_2O 9:1, v/v) R_t/min 3.8; $[\alpha]_D^{29}$ −22.2 (*c* 1.1 in CH_3OH); λ_{max}(CH_3OH)/nm 280 (ε/dm^3 mol^{-1} cm^{-1} 75); $\Delta\varepsilon_{293}$ −1.31; ν_{max}(nujol)/cm^{-1} 1705 (C=O), 3318, 3525 and 3626 (OH); *m*/*z* 430 (M^+ − 18, 1%), 387 (M^+ − 61, 3), 359 (M^+ − 89, 2), 348 (M^+ − 100, 100); δ_H and δ_C see Table 1.

X-Ray crystallography of 4

Crystal data. $C_{28}H_{48}O_4$ $M = 448.66$, orthorhombic, space group $P2_12_12_1$ (No. 19), $Z = 4$, $a = 7.896(2)$, $b = 11.486(2)$, $c = 28.835(6)$ Å, $V = 2615.0(9)$ Å^3 (by least square refinement of 5000 reflections), $\lambda = 0.71069$ Å, colourless crystals, $\mu = 0.074$ mm^{-1}, $\rho_{calc.} = 1.14$ g cm^{-3}.†

Data collection and processing. STOE-IPDS diffractometer, graphite monochromated Mo-Kα radiation; 15893 reflections measured ($1.91 \leqslant \theta \leqslant 23.98°$) at room temperature, 4080 independent reflections ($R_{int} = 0.044$).

Structure analysis and refinement. Direct methods with the program SHELXS-86,[7] full-matrix least square refinement with the program SHELXL-93,[8] all non-hydrogen atoms anisotropic, the weighting scheme $w = 1/[\sigma^2(F_o) + (0.0479F_o)^2]$. Final *R* values [$I > 2\sigma(I)$] are $R_1 = 0.0314$, $wR_2 = 0.0719$.

NMR experiments

All ^{1}H and 2D NMR spectra were recorded at 295 K on a Varian UNITY500 spectrometer operating at 499.84 MHz for ^{1}H using a NALORAC 3 mm microsample inverse detection probe; ^{13}C {^{1}H} and APT NMR spectra were recorded on a Varian GEMINI300 (**3**) at 75.50 MHz and a Varian UNITY500 at 125.70 MHz (**4**). For ^{1}H and 2D NMR experiments, solutions of 3.9 mg of **3** and 1 mg of **4**, respectively, in 0.160 ml of $CDCl_3$ were used; for ^{13}C and APT experiments, solutions of 3.9 mg of **3** in 0.160 ml of $CDCl_3$ and 3.5 mg of **4** in 0.60 ml of $CDCl_3$ (+ some drops of CD_3OD) were used. Chemical shifts were referenced to internal TMS ($\delta = 0$, ^{1}H) and $CDCl_3$ ($\delta = 77.0$, ^{13}C), respectively. Samples for NOE measurements were carefully degassed by four freeze–thaw cycles and then flame-sealed under an argon atmosphere.

All experiments were carried out using standard pulse sequences given by the manufacturers. DQFCOSY, NOESY and gradient supported HSQC spectra were recorded and processed in the phase-sensitive mode with quadrature detection in both dimensions; gradient supported HMBC spectra were processed in absolute value mode.

Determination of inter-proton distances

In order to relate NOESY cross peak intensities to internuclear distances of the dipolar coupled proton pairs, NOESY spectra

† Atomic coordinates, bond lengths and angles, and thermal parameters have been deposited at the Cambridge Crystallographic Data Centre (CCDC). Any request for this material should quote the reference number 188/150. See http://www.rsc.org/suppdata/p2/1999/233 for crystallographic files in .cif format.

with a 500 ms mixing time were processed for both compounds with the NMR TRIAD program (SYBYL 6.4 software package, TRIPOS, St Louis, MO, USA). In both dimensions a 90° shifted squared sine bell window function was applied and the F1 dimension was zero-filled up to 2K data points. In the F2 dimension a fourth-order polynominal baseline correction was used. Cross peaks which would be important for the determination of side chain conformations were integrated with manually determined baseline and peak boundaries. In cases where cross peaks appeared as resolved multiplets, they were integrated separately and added up.

A complete relaxation matrix analysis program, MARDIGRAS[9–11] as implemented in SYBYL 6.4, was used to obtain inter-proton distances. In a first step, all side chain NOE intensities, except the NOEs of Me-26 and Me-27 (not yet stereospecifically assigned), and additionally for calibration some well resolved NOEs belonging to protons of the steroidal skeleton with fixed and known distances were used as program input. To avoid errors in NOE intensities due to *J* coupling NOEs and distances between the angular methyl groups 18 and 19 and β-axial oriented protons of the steroidal skeleton were used for distance calibration instead of geminal protons. With the obtained distance range constraints the stereospecific assignment of the prochiral methyl groups Me-26 and Me-27 could be done in a first molecular modelling step (high-temperature restraint molecular dynamics, see below). Subsequently, a second MARDIGRAS distance computation with the new molecular input structure and all side chain NOE intensities, including those of the diastereotopic methyl groups, was performed.

Molecular modelling

All molecular mechanics calculations were carried out on Silicon Graphics workstations using the TRIPOS force field[12] of the molecular software package SYBYL 6.4.

To obtain the prochiral assignment for Me-26 and Me-27, high temperature restrained molecular dynamics simulations were utilized. The first derived set of NMR upper and lower distances were added to the force field as pseudo-quadratic potentials with a force constant of 25 kcal mol^{-1} Å^{-2}. The simulation temperature and length were 1000 K and 100 ps, respectively; an NTV ensemble, an integration time step of 0.5 fs and a Boltzmann distribution of starting velocities were used. A non-bonded cut-off of 8 Å for van der Waals interactions was applied and non-bonded lists were updated every 5 fs. No electrostatic interactions were considered at this point. For both compounds, 100 conformations were extracted from the trajectory and energy minimized using the Powell method[13] until a gradient of 10^{-3} kcal mol^{-1} Å^{-1} was achieved.

For further refinement, both brassinosteroids were surrounded with ~670 chloroform solvent molecules (precomputed solvent box, 44.5 Å length in each dimension) and restrained energy minimization with the full set of distance range constraints (force constant 75 kcal mol^{-1} Å^{-2}) for 5000 Powell steps was perfomed. Partial charge contributions were calculated using the method of Gasteiger and co-workers[14,15] and electrostatic interactions were taken into account by using a constant relative permittivity (dielectric function) with $\varepsilon = 1$. Periodic boundary conditions were applied. Subsequently, the molecular ensembles were subjected to restrained molecular dynamics simulations at 300 K for 100 ps. The force field set-up and molecular dynamics parameters were identical with those of the energy minimization and the high-temperature simulations, respectively. From the trajectories 5 conformations of **3** and **4** were selected manually, relating to different values of side chain dihedral angles. The whole molecular ensembles, including both the steroid and all solvent molecules, were energy minimized to a gradient of less than 10^{-3} kcal mol^{-1} Å^{-1}.

In order to check whether the obtained conformations are stable without NMR-derived distance constraints concerning the TRIPOS force field, additional energy minimization of the conformations without distance restraints were performed.

Simulated annealing calculations in vacuum without restraints were carried out over 200 cycles to 1000 K over 1 ps and annealed to 300 K over 1 ps with an exponential function. The obtained 200 conformations were minimized (Powell method) with a constant relative permittivity (dielectric function) of $\varepsilon = 5$ (for chloroform) over 5000 steps to a gradient of less than 10^{-3} kcal mol^{-1} Å.

Results and discussion

Synthesis

Upon treatment with *m*-chloroperbenzoic acid, (24*R*)-3β-hydroxy-24-methyl-5α-cholest-22-en-6-one, prepared in 5 steps from ergosterol,[16] was transformed to a 1:1 mixture of the (22*S*,23*S*)- and (22*R*,23*R*)-epoxides **5** and **6**.[6] Acid catalyzed *trans*-opening of the epoxide ring under addition of water yielded a mixture of the two vicinal diols (22*S*,24*R*)-teasterone (**3**) and (23*S*,24*R*)-teasterone (**4**) (see Scheme 1), separable by preparative HPLC (see Experimental section). Compound **4** easily gave X-ray quality crystals from acetone–n-hexane. X-Ray analysis of **4** indicated a (22*R*,23*S*) configuration of the vicinal diol function. Thus, compound **3** has to have the (22*S*,23*R*) configuration. Starting from the separated epoxides **5** and **6**, acid catalyzed water addition gave also mixtures of the bisepimeric compounds **3** and **4** in a ratio of 0.8:1 and 0.7:1, respectively, as detected by HPLC.

NMR resonance assignment

As a first step, all ^{1}H and ^{13}C resonances were unequivocally assigned by the combined use of 1D and 2D experiments (including DQFCOSY, GHSQC and GHMBC) as described in previous papers.[4,17,18] The distinction of α- and β-faced protons of the steroidal skeleton was done by 1D NOE difference experiments with irradiation of the two β-angular methyl groups Me-18 and Me-19 and assisted by inspection of coupling patterns of HSQC cross peaks. The ^{1}H and ^{13}C chemical shifts of **3** and **4** are given in Table 1.

NOE measurements and assignment

NOESY spectra were recorded with a mixing time of 0.5 s for both compounds **3** and **4** in order to avoid spin-diffusion artifacts. The assignment of 2D NOESY cross peaks suffers from the small dispersion of the ^{1}H chemical shifts of the methyl groups and signal overlap in the alkyl resonance region. However, benefitting from the high digital resolution of 1D NOE difference spectra, nearly all the ambiguities in NOE assignments could be cleared up. In the case of **3**, irradiation of the H-22 and H-23 resonances, respectively, allowed the unambiguous assignment of the NOEs of H-22 to H-16α, H-16β, H-25 and Me-28 and of H-23 to all four side chain methyl groups.

The two ^{1}H methyl doublets of Me-26 and Me-28 form a "*quasi*-triplet" because the high-field line of Me-26 and the low-field line of Me-28 are superimposed. Irradiation of each of the three lines with very low power gave distinct differences in the resulting NOE difference spectra and thus the NOEs could be assigned to those caused by spatial proximity to Me-26 and those which are due to Me-28. Me-26 shows a strong NOE interaction with H-24 and a medium one with H-23, whereas H-23 gives a strong NOE with Me-28 and H-22 a weak NOE with this methyl group (Fig. 1).

In the case of **4** selective decoupling of the Me-26 and Me-27 doublets during the acquisition time of the NOE difference experiment allowed the assignment of NOEs to the nearly isochronous signals of H-24 and H-25, respectively, since only the signal shape of H-25 is collapsed. However, concurrent NOE correlations of H-24 and H-25 could not be integrated

Table 2 Selected NOE correlations of compounds **3** and **4**[a,b]

3	H-20	Me-21	H-22	H-23	H-24	H-25	Me-28	Me-26^{proR}	Me-27^{proS}	H-12β	H-16α	H-16β	H-17α	Me-18
H-20			w											s
Me-21			w	s						s			s	s
H-22	w	w		?		s	w				m	m		
H-23		s	?		s		s	w	w					
H-24				s		?			s					
H-25			s		?									
Me-28			w	s				?	?					
Me-26^{proR}				w			?							
Me-27^{proS}				w	s		?							
Me-18	s	s								s		s		
4	H-20	Me-21	H-22	H-23	H-24	H-25	Me-28	Me-26^{proR}	Me-27^{proS}	H-12β	H-16α	H-16β	H-17α	Me-18
H-20			s	w										s
Me-21				s			?			s			s	s
H-22	s			?	m	m	s				s	s	w	
H-23	w	s	?		m	s	w	s	w					
H-24			m	m		?		?	w					
H-25			m	s	?		s							
Me-28			s	w		s		?	m					
Me-26^{proR}				s	?		?							
Me-27^{proS}				w	w		m							
Me-18	s	s								s		s		

[a] Trivial NOEs between methyl protons and their vicinal protons are not noted. [b] s, strong NOE; m, medium NOE; w, weak NOE; ?, owing to insufficient dispersion of chemical shifts or an artifact in the spectrum it is impossible to determine whether a NOE exists or not.

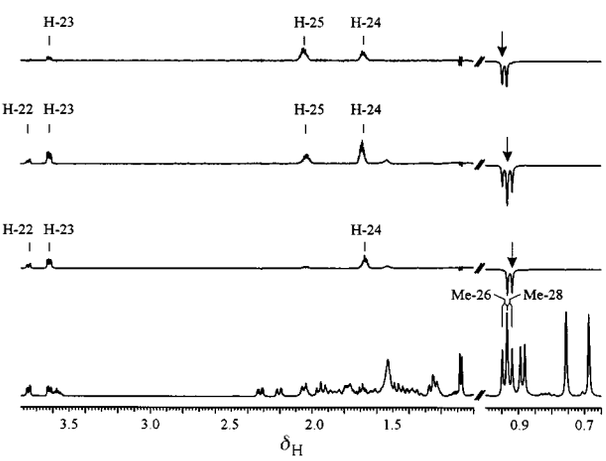

Fig. 1 500 MHz ^{1}H NOE difference spectra of 22,24-diepiteasterone (**3**) in $CDCl_3$ with selective irradiation of the doublet lines of Me-26 and Me-28. The lower trace is the routine ^{1}H NMR spectrum. NOE irradiation frequencies are marked by arrows. Vertical and horizontal scales of the left and right part of spectra are different.

separately and thus these NOEs could be utilized only on a qualitative level. A summary of all relevant side chain NOE contacts found for **3** and **4** is given in Table 2. The differences in NOE correlation pattern for **3** and **4** suggest the existence of different preferential solution side chain conformations for both compounds.

Conformational analyses

In order to convert integral intensities of NOESY cross-peaks into distance range information a complete relaxation matrix analysis method which takes into account fast methyl rotation was used (MARDIGRAS as implemented in SYBYL 6.4, see Experimental section). In the case of **3** a starting model structure was built with the SYBYL graphical interface, whereas in the case of **4** the X-ray structure could be used. In a first MARDIGRAS run NOEs belonging to the diastereotopic methyl groups Me-26 and Me-27 were ignored, because they were not yet assigned. With the obtained distance ranges a restrained molecular dynamic simulation was performed (for details see Experimental section). After energy minimization of

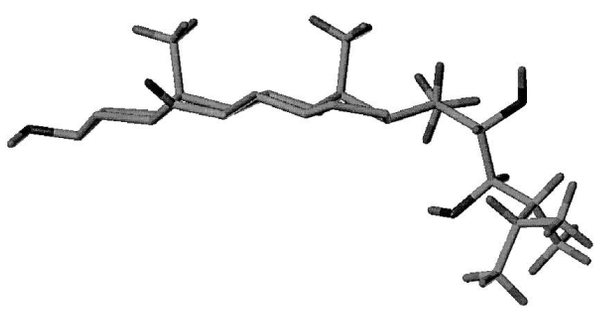

Fig. 2 NOE supported solution conformation of 22,24-diepiteasterone (**3**) (only side chain protons are shown).

the obtained structures 5 conformational families were found for **3** and 3 conformations for **4**. However, in each case only one conformational family was in agreement with the experimental NOE contacts belonging to the geminal methyl groups Me-26 and Me-27. Thus, an assignment of the diastereotopic methyl groups Me-26$^{pro\text{-}R}$ and Me-27$^{pro\text{-}S}$ was possible for **3** and **4**. For **3**, the assignment was made using the strong NOE between the geminal methyl group at δ 0.942 (Me-27^{proS}) with H-24, and for **4** the methyl group at δ 0.966 could be assigned to Me-26^{proR} because of its strong NOE with H-23. In a second MARDIGRAS run the NOE contacts belonging to Me-26 and Me-27 were included and a complete set of distance ranges was obtained.

With the full set of distance ranges a further molecular dynamics simulation was carried out for **3** and **4** considering a $CHCl_3$ solvent box of 45 Å length in each dimension. For each case 5 snapshots were selected from the dynamics trajectory. Energy minimization taking all solvent molecules into account led to a structure for **3** (Fig. 2) and **4** (Fig. 3) with only a few violations of NOE restraints: for **3**, the distance of the calculated conformation H-23/Me-27 of 5.0 Å is somewhat too long for the observed weak to medium NOE. However, the dynamics simulations showed a fluctuation between 4.55 to 5.11 Å for this distance. For **4**, the NOEs between Me-28 and the two geminal methyl groups 26 and 27 are not in full agreement with the corresponding distances of the calculated conformation. However, in the only conformation which satisfies these NOEs, the NOE constraint H-25/Me-28 is violated. Since NOEs

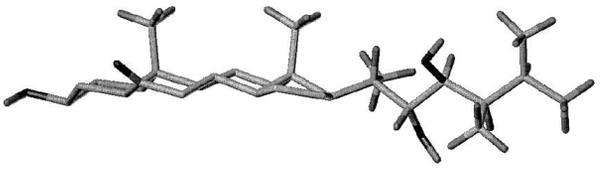

Fig. 3 NOE supported solution conformation of 23,24-diepiteasterone (**4**) (only side chain protons are shown).

between methyl groups are more uncertain, their violations are acceptable.

In order to prove whether the calculated structures are energetically stable ones, an energy minimization including the solvent but without any restraints was done. In both cases **3** and **4** the conformations underwent no significant conformational changes. However, **4** showed a slightly different conformation when it was minimized without restraints in vacuum, whereas for **3** it had no effect on the obtained conformation whether the solvent was taken into account or not in the course of energy minimization. Molecular dynamic calculations taking into account the solvent but with no restraints gave nearly the same conformation for **3** and **4** as did the restrained calculations. This finding proves the obtained conformations to be stable and low-energy ones with respect to the force field used.

In addition, simulated annealing calculations (for details see Experimental section) were performed in order to test whether the whole conformational space was analyzed. All obtained 200 conformations were minimized and the carbon atoms of the steroidal skeleton were fitted to those of the NOE supported preferred conformations. For **3** and for **4**, the conformation with the best fit differs not more than 3 kcal mol^{-1} from the lowest-energy conformation of the simulated annealing run. Thus, the NOE supported solution conformations of **3** and **4** are energetically stable ones.

In both cases **3** and **4**, in the preferred solution conformation, yielded by NOE restrained molecular dynamic calculations, the hydroxy groups at C-22 and C-23 show an *anti* relationship. The same is true for H-22 and H-23. This is supported by the vicinal coupling constant $J_{\text{H-22/H-23}}$ of *ca.* 8 Hz in the case of **3** and **4**. The angle H-22–C-22–C-23–H-23 of the calculated conformation is −164° and −168° for **3** and **4**, respectively. Thus, for the side chain hydroxy groups no hydrogen bonds are observed. The side chain of **4** is more stretched in comparison with that of **3**, which shows a kink at C-22. The wide difference of $\Delta\delta_{\text{C-20/C-25}}$ with 15.4 and 5.5 for **3** and **4**, respectively (see Table 1) can be explained by a shielding γ-*gauche* effect of OH-23 on C-25, but not C-20 for **3** on the one hand and just the opposite for **4** on the other hand.

For **4**, the solid state conformation was determined by X-ray analysis (Fig. 4). Three intermolecular hydrogen bonds are observed in the crystal lattice to have a strong influence on the side chain conformation, which differs significantly from that found in solution (Fig. 5). Hence, the calculated proton–proton distances ‡ of the X-ray structure are not in accordance with the NOEs observed in solution. For example, the distance H-20/H-25 for the X-ray structure is 2.4 Å, but no NOE was detected for these two protons. On the other hand, a strong NOE contact was found for Me-21/H-23 and H-22/Me-28. However, the corresponding distances of the X-ray structure are 4.5 and 4.6 Å, respectively, whereas for the calculated conformation, these distances are 3.3 and 3.2 Å, respectively, and thus are in agreement with the strong NOEs detected. The calculated volume of **4** for the conformation in the crystal is 441 $Å^3$ but for the solution conformation is about 447 $Å^3$. This difference indicates that, on the one hand, crystal packing effects lead to the adoption of the solid phase conformation with lower volume than in the solution conformation. On the other hand, the slightly higher volume of the calculated solution conformation is probably caused by enhanced entropy content.

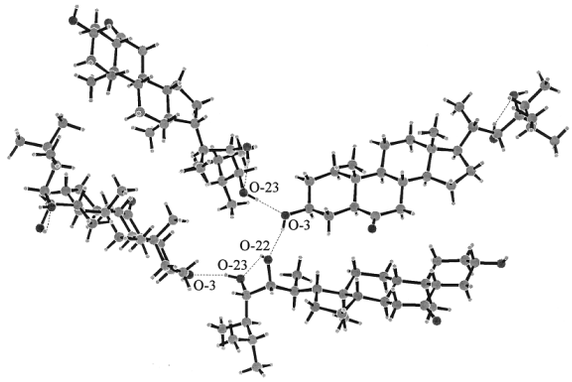

Fig. 4 Orientation of the molecules of 23,24-diepiteasterone (**4**) in the crystal. Hydrogen bonds are shown by dashed lines.

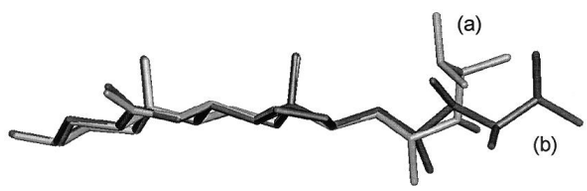

Fig. 5 Comparison of (a) the X-ray conformation and (b) the calculated solution conformation of 23,24-diepiteasterone (**4**) (for clarity protons are not shown).

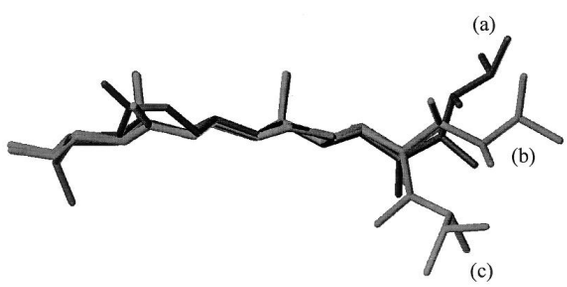

Fig. 6 Comparison of the calculated solution conformations of (a) brassinolide (**1**), (b) 23,24-diepiteasterone (**4**) and (c) 22,24-diepiteasterone (**3**) (for clarity protons are not shown).

The conformation of the bioinactive brassinosteroid analogues **3** and **4** are both clearly different from that of the most bioactive brassinosteroid brassinolide (**1**) (Fig. 6).[4] For both **3** and **4**, the calculated energy of the molecule in a conformation similar to that found for brassinolide (**1**) is about 10 kcal mol^{-1} higher than the energy calculated for the NOE supported solution conformation. This should be due to steric compression of Me-28 and both H-16β and H-20 in the case of a brassinolide-like conformation.

Conclusions

Two new brassinosteroid analogues, 22,24-diepiteasterone (**3**) and 23,24-diepiteasterone (**4**) were synthesized and their solution conformations investigated by quantitative NOE measurements and restrained molecular dynamics simulations. The two bioinactive compounds show different preferred conformations in solution. Neither of them resembles the side chain conformation of the most bioactive brassinosteroid brassinolide (**1**), reflecting the high importance of the stereochemistry of this structural feature for the interaction with a putative receptor. Furthermore, for **4**, the conformation in the

‡ For better comparability distances and volumes of the X-ray structure and the calculated solution conformation of **4** discussed in this paragraph are both calculated using the TRIPOS SYBYL 6.4 software package. For that purpose the coordinates of a molecule of the X-ray structure were imported into SYBYL.

crystalline state was determined by X-ray analysis. The obtained structure differs from that in solution which is mainly due to intermolecular hydrogen bonds in the crystal.

Acknowledgements

We gratefully acknowledge the financial support by the Deutsche Forschungsgemeinschaft (grant Po 581/1–1).

References

1 H. G. Cutler, T. Yokota and G. Adam (Eds.), *Brassinosteroids—Chemistry*, *Bioactivity*, *Applications*, *ASC Symposium Series*, American Chemical Society, Washington DC, 1991, vol. 474.
2 G. Adam, A. Porzel, J. Schmidt, B. Schneider and B. Voigt, in *Studies in Natural Products Chemistry*, ed. Atta-ur-Rahman, Elsevier, Amsterdam, 1996, vol. 18, p. 495.
3 T. Yokota and K. Mori, in *Molecular Structure and Biological Activity of Steroids*, eds. M. Bohl, W. L. Duax, CRC Press, Boca Raton, FL, 1992, p. 318.
4 M. Stoldt, A. Porzel, G. Adam and W. Brandt, *Magn. Reson. Chem.*, 1997, **35**, 629.
5 B. Voigt, unpublished work.
6 B. Voigt, A. Porzel, C. Bruhns, C. Wagner, K. Merzweiler and G. Adam, *Tetrahedron*, 1997, **53**, 17039.
7 G. M. Sheldrick, SHELXS-86, A program for structure solution 1986, University of Göttingen.
8 G. M. Sheldrick, SHELXL-93, A program for crystal structure refinement 1986, University of Göttingen.
9 B. A. Borgias and T. L. James, *J. Magn. Reson.*, 1990, **87**, 475.
10 B. A. Borgias, M. Gochin, D. J. Kerwood and T. L. James, *Prog. Nucl. Magn. Reson. Spectrosc.*, 1990, **22**, 83.
11 H. Liu, P. D. Thomas and T. L. James, *J. Magn. Reson.*, 1992, **98**, 163.
12 M. Clark, R. D. Cramer, III and N. van Opdenbosch, *J. Comput. Chem.*, 1989, **10**, 982.
13 M. J. D. Powell, *Math. Programming*, 1977, **21**, 241.
14 J. Gasteiger and M. Marsili, *Tetrahedron*, 1980, **36**, 3219.
15 J. Gasteiger and H. Saller, *Angew. Chemie*, 1980, **97**, 699.
16 B. Voigt, J. Schmidt and G. Adam, *Tetrahedron*, 1996, **52**, 1997.
17 A. Porzel, V. Marquardt, G. Adam, G. Massiot and D. Zeigan, *Magn. Reson. Chem.*, 1992, **30**, 651.
18 T. Ando, M. Aburatani, N. Koseki, S. Asakawa, T. Mouri and H. Abe, *Magn. Reson. Chem.*, 1993, **31**, 94.

Paper 8/07440B